The Characterisation of Diesel Cavitating Flow using Time-Resolved Light Scattering

R.D. Lockett, L. Liverani, D. Thaker, C. Arcoumanis
School of Engineering & Mathematical Sciences
City University London
Northampton Square, EC1V 0HB
London, UK

ABSTRACT

A conventional six-hole valve-covered orifice (VCO) injector nozzle has been modified in order to provide optical access to the region below the needle, and the nozzle passages. This has been achieved through the removal of the metal tip, and its replacement with a transparent acrylic tip of identical geometry.

Elastic scattering of light obtained from the internal cavitating flow inside the nozzle holes of the optically accessible diesel injector tip was captured on a high speed electronic camera. The optical image data was obtained from a nozzle with a common rail pressure of 400 bar, and for two diesel fuels, in order to identify differences in cavitation behaviour.

A set of 100 mean diesel fuel injection images were obtained from 30 fuel injection pulses, for each operating condition. The imaged mean cavitation occurring in the nozzle holes was converted to the mean proportion of nozzle hole area producing cavitation scattering. The mean cavitation area images were then analysed, and were able to demonstrate the inverse relationship between fuel mass injected and the relative area producing cavitation scattering.

Key Words: diesel nozzle flow, cavitation, VCO diesel injector, elastic light scattering, imaging.

1 INTRODUCTION

Modern common rail direct injection diesel engines operate through the injection of high pressure liquid diesel fuel into the engine combustion chamber. The fuel is normally injected through a number of nozzle holes located at the base of an injector. The liquid fuel is subjected to large pressure gradients inside the injector and the nozzle passages, which often causes local boiling of the fuel to create local pockets of fuel vapour. This type of flow is called cavitating flow, and is associated with unstable, unsteady vapour cavities forming inside the flowing fuel.

Several groups have identified the likelihood of cavitation occurring in the internal fuel flow inside these injector nozzles[1–3]. Internal cavitating flow occurring inside fuel injectors is believed to produce a number of effects on the internal fuel flow and the injector such as those listed below:

(1) Nozzle cavitation reduces the injected fuel mass in an unpredictable manner, which can result in poor fuel/air mixture formation in the engine, unstable combustion and/or higher engine-out emissions [4–8].
(2) Nozzle cavitation affects the atomisation of the fuel jets into droplets as the jets [2,9,10].
(3) Cavitation may cause surface erosion and, ultimately injector failure [11].
(4) Cavitation may induce chemical changes in the fuel, resulting in either the formation of internal deposits [12] or the prevention of such deposits.

Recent research in cavitation flow relevant to high pressure diesel injection systems has developed in two complementary directions, which are firstly, the characterisation of cavitation flows in large scale injectors that offer full optical access, and secondly, studies of cavitation occurring in real size injectors under realistic operating conditions.

Two clearly distinguishable types of cavitating flow have been identified in large scale nozzle studies. These are geometric-induced cavitation and vortex or string cavitation. Geometric cavitation forms at orifice inlets and it is due to the abrupt acceleration of the fuel flow as it enters the nozzle holes. The local pressure gradient gives rise to conditions that facilitate local boiling. Geometric cavitation appears to be initiated as a dense foam of micro-bubbles developing in the liquid phase, which evolves into a connected volume of fuel vapour running from the

hole inlet to the hole exit. On the other hand, string cavitation is a highly transient phenomenon which occurs inside the nozzle sac volume. They appear as thin strings of fuel vapour, usually connecting two adjacent holes. They are associated with low pressure regions where the local flow is subjected to large vorticity such as the vortex core [13–19].

Geometric cavitation and string cavitation have both been observed in optically accessible real-size injectors [20–26], confirming previous studies in large scale transparent model injectors.

It is interesting to note that a number of experiments have been conducted on biodiesel injection, atomisation and mixing in diesel engines [27,28]. Their authors have reported that the spray characteristics of biodiesel are somewhat different to those of conventional diesel, and have suggested that the susceptibility of biodiesel to develop internal cavitation flow may be lower than conventional diesel fuel.

The objective of this work was to establish whether it was possible to identify whether different diesel fuels produced different cavitation flow inside the injector nozzles. In order to achieve this, it was necessary to obtain time-resolved elastic back-scattering images of cavitation occurring within the nozzle passages of an optically accessible Valve-Covered-Orifice (VCO) injector operating near realistic injection conditions. The time-resolved back-scattered images obtained from the cavitating diesel in the nozzles were assumed to be approximately proportional to the local surface area defining the boundary between the liquid and vapour present in the flow.

2 EXPERIMENTAL ARRANGEMENTS

2.1 The Optically Accessible Injector

A conventional VCO injector had its metal tip (including the nozzle holes) machined off. The replacement optically accessible acrylic injector tip was manufactured by hand at City University's engineering workshop, reproducing the exact internal geometry of the VCO nozzle tip. A schematic of the arrangement is shown in Figure 1. It is important to note that the acrylic tip attached to the injector below the needle seat, ensuring that the acrylic tip did not suffer any damage during needle opening and closure.

The injector was mounted in a hollow cylindrical frame constructed from steel. The injector was fixed in a hole at the top end of the cylindrical frame. The acrylic tip was held in place with a transparent acrylic disc of approximately 10 mm thickness and 40 mm diameter. The acrylic disc was mounted on a pre-loaded sprung steel ring with an open centre. The adjustable compression force exerted on the tip by the disk ensured that the tip could withstand up to 600 bar rail fuel pressure without leaking.

The diesel fuel was injected through the nozzle holes in the injector tip into atmospheric air in the laboratory. Consequently, an air extraction facility was placed adjacent to the injector in order to protect personnel from exposure to atomised diesel fuel within the laboratory space.

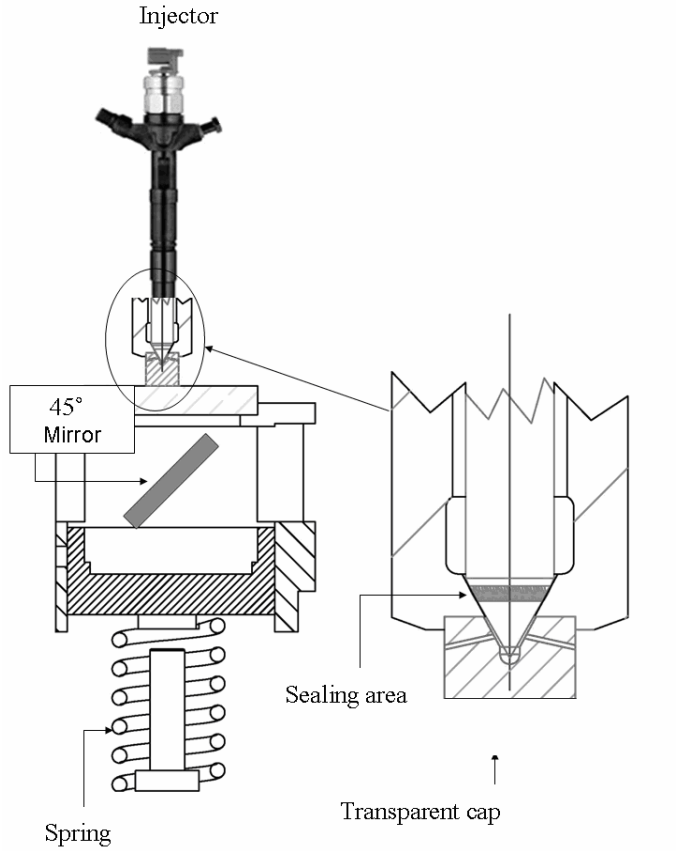

Figure 1 - Mounting Configuration of the Optically Accessible VCO Injector

2.2 The Fuel Injection System

The modified injector was connected to a Denso high pressure diesel common rail injection system. The prototype electronic fuel injection system enabled user control of the common rail pressure and the injection timing and duration. The injection parameters

were controlled from a personal computer equipped with National Instruments data control cards, which controlled the electronic injector driver. The electronic injector driver sent a high voltage square wave pulse to a magnetic solenoid, located in the injector. The switching of the magnetic solenoid actuated the injector needle, allowing high pressure fuel to pass through the injector. The mean time-resolved needle lift for this type of injector was measured using an inductive sensor, and is shown on the timing diagram presented in Figure 2.

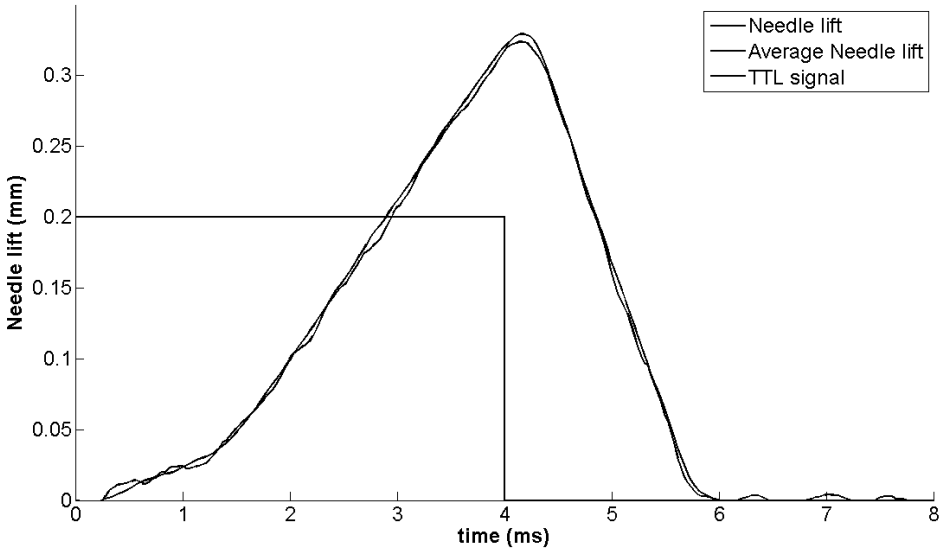

Figure 2 – Graph of Needle Lift and Injection Pulse versus Time.

Figure 2 shows a graph of the measured needle lift versus time on the same axes as the injection pulse. The needle lift profile is rather unusual, in that the needle lift rate is smaller than expected. This was due to the relatively low common rail pressure of 200 bar to 400 bar. The injectors employed in this study were designed for rail pressures of approximately 1200 bar to 1600 bar. Once the needle begins to retract, the high fuel pressure facilitates the development of a large needle lift rate. The needle normally reaches its highest point within 0.5 ms, and remains open until the magnetic circuit is turned off. In this set of experiments, the needle took 4 ms to reach its highest point, at which time the solenoid switched off, and the needle returned to its seating position. The needle return took another 1.5 ms to 2 ms to complete.

A variable speed motor was employed to drive a Denso diesel common rail pump. A laptop computer was employed to control a prototype programmable electronic control unit, which in turn, controlled the fuel pressure in the common rail. The diesel fuel temperature could be controlled by passing the diesel fuel through a heat exchanger sited between the fuel tank and the high pressure pump, although this facility was bypassed in these experiments.

2.3 The Optical Arrangement

The optical arrangement is shown in Figure 3. Continuous white light obtained from a collimated Arri 400 W lamp was passed though a 150 mm diameter glass lens with 25 cm focal length. The focussed light was reflected up though the hollow metal tube using a 45 deg mirror. The light was further focussed onto the acrylic tip, by passing it through an infra-red filter and a 40 mm diameter lens with 50 mm focal length, followed by a beam splitter plate arranged at 45 deg.

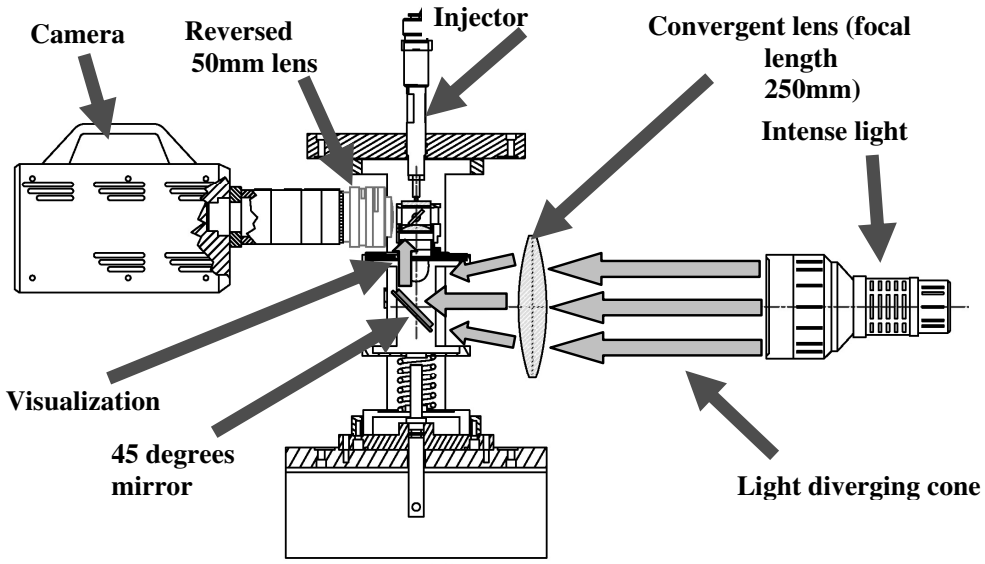

Figure 3 - Schematic of Optical Arrangement

Back-scattered light obtained from the cavitating diesel in the nozzle passages was reflected onto a high speed Photron Ultima APX–RS video camera using a Nikon 50 mm f1.2 camera lens, reverse coupled to 60 mm lens extension tubes. This arrangement facilitated high resolution imaging of approximately 10 μm/pixel. The Photron APX–RS camera was configured to obtain 512 pixel x

512 pixel images at 10 kHz. The use of this camera in this manner facilitated real-time capture of individual injection events.

The camera was configured to begin capturing images synchronous with the leading edge of the electronic pulse sent to the injector. On receipt of the injector pulse, the camera took 100 frames at 10 kHz frame rate for 10 ms duration. Each frame had an exposure duration of 1.0 μs. In order to protect the camera and the camera lens from exposure to atomised diesel oil, absorbent paper was placed around the injection region.

3 EXPERIMENTAL METHODOLOGY

The main objective of the experiment was to determine whether different diesel fuel samples produced identifiably different cavitation inside the nozzle holes. In this regard, two diesel fuel samples were employed in this study. One of the samples was a prototype diesel (Fuel A), while the other was a bio-diesel (Fuel B).

Modern high pressure common rail diesel injection systems operate at pressures of between 1400 bar and 2000 bar. Due to the properties of acrylic, the maximum operating rail pressure that could be achieved during this study was 400 bar. Operating at lower pressure therefore required longer injection duration in order to inject a comparable quantity of diesel.

It was considered desirable to examine the internal flow during needle lift and return, and steady-state maximum lift. Consequently a fixed fuel injection pulse of 4 ms was employed for all tests. The needle lift and the injector pulse are shown in Figure 2.

It was observed that the acrylic injector tips experienced significant erosion when subjected to multiple injections of fuel at 400 bar rail pressure. The ongoing erosion of the acrylic surface at the inner entrance to the nozzle holes caused the cavitation flow inside the nozzle passages to change over time. These changes were assessed over time by subjecting a small number of test injector tips to approximately 1000 injections each at 400 bar rail pressure. Based on the cavitation behaviour, an injector lifetime of approximately 200 injections was conservatively estimated when injecting at 400 bar rail pressure.

An experimental session combining a new injector tip with a single fuel consisted of firstly obtaining 40 background images of the

injector tip containing 100 % liquid fuel, followed by obtaining 30 sets of 100 images synchronous with 30 injections at 400 bar, 300 bar and 200 bar respectively.

Following each experimental session, the mean injected fuel mass was measured for each diesel fuel sample. This was achieved by firstly changing the optical accessible injector with a conventional one, followed by injecting the diesel fuel sample though the conventional injector for 1000 injections into a sealed receiving vessel. The number of injections was electronically counted. The mean injected mass was determined by dividing the net mass of fuel by the total number of injections. The results of these measurements are presented in Table 1.

Table 1 - Injected Fuel Mass for Tested Diesel Samples

Fuel type	**Density (g/cm^3)**	**Fuel mass per injection (mg)**	**Mass Flow Rate (g/sec)**	**Volumetric Flow Rate (cm^3/s)**
FUEL A	0.82 (est.)	54.63	13.66	16.53
FUEL B	0.83	55.40	13.85	16.60

The diesel fuel required changing following an experimental session. The fuel system was drained, and then refilled with the new diesel fuel sample. This fuel sample was passed through the system, and then drained. This was defined as one flush. The fuel system was flushed in this manner four times, before the new fuel was used for the next experimental session. This flushing process ensured that less than 1 % of the original diesel fuel remained in the system from session to session.

4 IMAGE PROCESSING

Each experimental session involved the injection of one of the diesel fuel samples into laboratory air, using 400 bar common rail pressure. The camera was configured to capture 100 time-resolved images of the internal cavitating flow at 0.10 ms intervals for 10 ms duration, for each injection. Image data was obtained from 30 injections, making a total of 3000 images per fuel sample.

Each set of 3000 images were numbered frame 1 to frame 3000. Frames 1, 101, 201, 301, 401 … 2901 made up a subset of 40 images of the diesel fuel inside the injector passages obtained at 0.1 ms after the leading edge of the start-of-injection (ASOI) electronic pulse. Frames 2, 102, 202, 302, 402 … 2903 made up a subset of 40 images obtained at 0.2 ms after the leading edge of the SOI pulse, and so on to the subset of images defined by frame 100, 200, 300 … 3000.

In order to express the processing of the data images mathematically, the pixel intensity on the raw data images is represented by S_{ij}^{klm}, where S_{ij}^{klm} represents the intensity of the pixel located on the CCD chip at the position defined by the row index *i* and the column index *j*, $i, j \in \{1,2,3,...512\}$. The index number *k* represents the frame number within a set of 100 time-resolved images for a single injection event, ranging from frame 1 to frame 100; while the index number *l* refers to the specific injection event, ranging from injection 1 to injection 30. The index number *m* refers to the diesel fuel sample tested, and ranges from 1 to 2, representing fuel samples A and B.

For each fuel sample and each rail pressure, a set of 100 mean time-resolved cavitation images were determined by finding the mean images associated with frames 1, 101, 201, 301 … 2901, frames 2, 102, 202, 302, … 2902, frames 3, 103, 203, 303, … 2903, and so on up to frames 100, 200, 300, … 3000. This is expressed mathematically by

$$\overline{S_{ij}^{km}} = \frac{1}{30}\sum_{l=1}^{30} S_{ij}^{klm} \quad . \qquad (1)$$

Standard deviation images were also computed from the above data. These are expressed by

$$X_{ij}^{km} = \sqrt{\frac{1}{29}\sum_{l=1}^{29}\left(S_{ij}^{klm} - \overline{S_{ij}^{km}}\right)^2} \quad . \qquad (2)$$

40 background images were obtained for each experimental session. These pixel intensity data are represented by the indexed intensity variable B_{ij}^{mp}, where the index numbers *i*, *j*, and *m* retain their meaning from above, while the index number *p* refers to

background image 1 to 40. A mean background image was calculated for each experimental session. This is expressed by

$$\overline{B_{ij}^{m}} = \frac{1}{40}\sum_{p=1}^{40} B_{ij}^{mp} \ . \qquad (3)$$

Processed data images were generated by subtracting the mean background images from the mean time-resolved cavitation images. These are expressed by

$$\overline{I_{ij}^{km}} = \overline{S_{ij}^{km}} - \overline{B_{ij}^{m}} \ . \qquad (4)$$

An example of this form of image processing is shown in Figure 4. In order to process the captured optical data properly from the raw data image (the image on the left of Figure 4), the background image must be subtracted (the middle image). The processed image on the right is the final image obtained after background subtraction.

The mean image frame intensity data defined by $\overline{I_{ij}^{km}}$ were subjected to a threshold test as to whether cavitation was present or absent. This consisted of setting pixel values to zero where the actual intensity was smaller than 10 % of the mean intensity. Mathematically, this is expressed by determining the image mean intensity

$$\overline{I^{km}} = \frac{1}{NM}\sum_{i=1}^{N}\sum_{j=1}^{M}\overline{I_{ij}^{km}} \ , \qquad (5)$$

and then applying the cavitation threshold test, expressed by the conditional

$$\text{If } \overline{I_{ij}^{km}} < \frac{\overline{I^{km}}}{10} \text{, then set } \overline{I_{ij}^{km}} = 0 \ . \qquad (6)$$

The mean image frame intensity data was then analysed in terms of ranges of signal intensity. The pixels were placed in 64 bins representing equal ranges of intensity from minimum to maximum. The bins were then integrated to obtain the total number of pixels producing cavitation scattering data. This

number was then divided by the total number of pixels in the nozzle passages to obtain the relative proportion of area within the imaged nozzle passage area producing optical scattering.

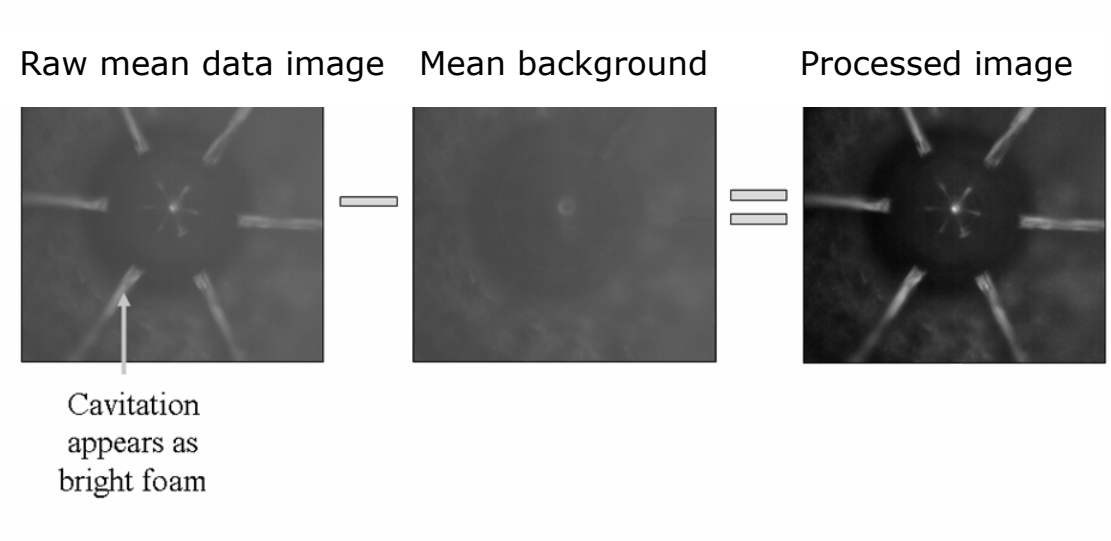

Figure 4 - Images showing Image Processing Methodology.

The mean time resolved, normalised, cavitation scattering area has been represented as histograms. A tenth order polynomial has been fitted to the histogram data in order to achieve the best possible polynomial fit. These graphs are presented in Figure 5.

5 RESULTS AND DISCUSSION

The right hand image in Figure 4 is an image of the mean cavitation scattering obtained from the cavitating flow occurring in the nozzle passages of the optically accessible injector tip after background subtraction. The optical scattering captured on the video camera was being back-scattered from the cavitating diesel fuel, and appears as the six bright streaks pointing away from the centre of the image.

Figure 5 shows the graphs of the time-resolved relative proportions of area within the injector nozzle passages producing back-scattered light as a result of diesel fuel cavitation, obtained at 400 bar rail pressure. It can be seen that fuel sample A produces consistently greater cavitation-induced optical scattering than fuel sample B. These results reveal an inverse correlation with the injected mass results from Table 1.

This confirms the hypothesis that cavitation occurring within the nozzle passages results in a reduced discharge coefficient as a

result of partially choking the liquid flow. Hence an increase in cavitation is likely to result in a lower discharge coefficient.

One of the diesel samples tested was a prototype diesel fuel (Sample A), while the other was a biodiesel fuel (Sample B). The time-resolved scattering data presented in Figure 5 suggests that the biodiesel sample produced significantly less cavitation scattering than the prototype diesel. This result suggests that the cavitation surface area is smaller for the biodiesel sample when compared with the prototype diesel sample.

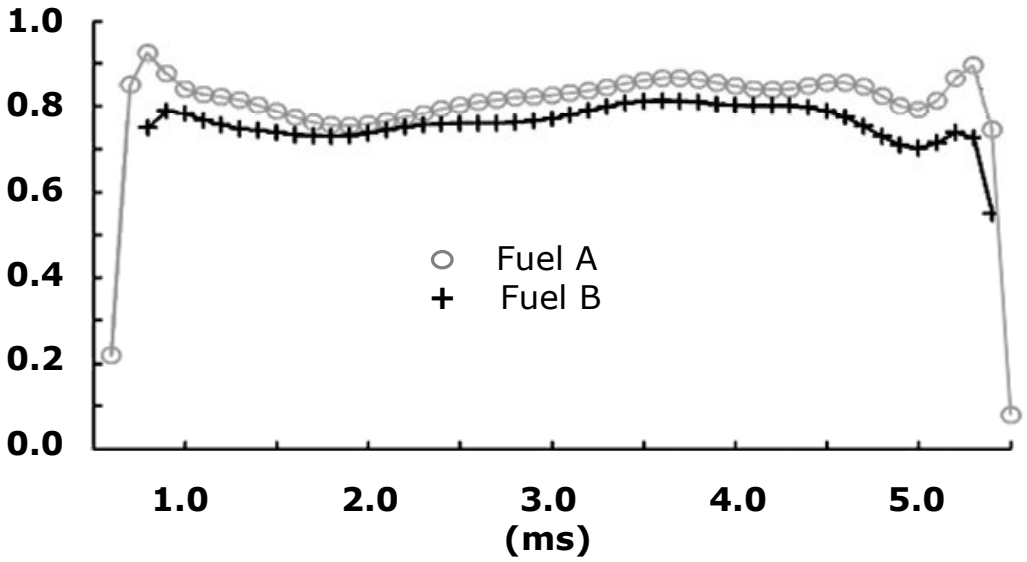

Figure 5 - Graphs of Relative Mean Cavitation Scattering Area as a Function of Injection Timing at 400 bar Rail Pressure.

6 CONCLUSIONS

A novel methodology that provides the ability to discriminate between the cavitation volume occupied by different diesel fuels during the fuel injection process has been developed and described. The methodology should also offer persuasive evidence of the correct link between occupied cavitation volume and injected fuel mass. Ideally the methodology should also be able to explain the relationship between occupied cavitation volume during fuel injection and the physical properties of the injected diesel fuel.

The experimental methodology reported here has been partially successful, in that the measurement data has been able to identify differences between the fuel samples through back-scattering of

light from cavitating flow, and is able to predict that elevated levels of cavitation in the nozzle passages results in reduced injected fuel mass.

Finally, it was observed that the biodiesel sample produced significantly less cavitation scattering than prototype diesel sample, suggesting that the biodiesel sample produced a smaller cavitation boundary surface area than the prototype diesel.

Further work is required in order to investigate whether this approach will be able to identify and correctly predict the dependence of the propensity of diesel to develop nozzle cavitation flow as a function of its physical properties.

ACKNOWLEDGEMENTS

The authors would like to acknowledge Shell Global Solutions for support for this project. In addition, the authors would like to acknowledge the valuable assistance of School of Engineering technical staff, particularly Jim Ford, Tom Fleming, Mike Smith and John Kenny.

REFERENCE LIST

1. Arcoumanis, C. and M. Gavaises, *Cavitation in diesel injectors: modelling and experiments.* Proceedings of the 14th ILASS-Europe Annual Conference, Manchester, England, 1998.

2. Kim, J.H., K. Nishida, H. Hiroyasu, *Characteristics of the Internal Flow in a Diesel Injection Nozzle.* ICLASS-97, 1997.

3. Soteriou, C., R. Andrews, M. Smith, *Direct Injection Diesel Sprays and the Effect of Cavitation and Hydraulic Flip on Atomization. .* SAE paper, 1995 (950080).

4. Soteriou, C., M. Smith, R.J. Andrews, *Cavitation Hydraulic Flip and Atomization in Direct Injection Diesel Sprays.* IMechE Paper C465/051/93, 1993.

5. Arcoumanis, C., M. Gavaises, J.M. Nouri, E. Abdul-Wahab, *Analysis of the flow in the nozzle of a vertical multi-hole diesel engine injector, .* SAE paper, 1998 (980811).

6. Soteriou, C., R. Andrews, M. Smith, N. Torres, S. Sankhalpara, *The Flow Patterns and Sprays of Variable Orifice Nozzle Geometries for Diesel Injection.* SAE paper, 2000 (2000-01-0943).

7. Desantes, J.M., R. Payri, F.J. Salvador, J. Gimeno, *Measurements of Spray Momentum for the Study of Cavitation in Diesel Injection Nozzles.* SAE paper, 2003 (2003-01-0703).

8. Payri, F., V. Bermudez, R. Payri, F.J. Salvador, *The influence of cavitation on the internal flow and the spray characteristics in diesel injection nozzles*. Fuel. Vol. 83. 2004, 419-431.

9. Nishida, K., S. Ceccio, D. Assanis, N. Tamaki, H. Hiroyasu, *Characterization of Cavitation Flow in a Simple Hole Nozzle.* ICLASS-97, 1997.

10. Soteriou, C., M. Smith, R. Andrews, *Diesel injection: laser light sheet illumination of the development of cavitation in orifices.* IMECHE conference transactions, 1998 (C529/018/98).

11. Osman A., *Failure of a diesel engine injector nozzle by cavitation damage*, Engineering Failure Analysis vol. 13 issue 7, October 2006, 1126 – 1133.

12. N. Tait, Shell Global Solutions, Personal Communication, 2008.

13. Arcoumanis, C., H. Flora, M. Gavaises, N. Kampanis, R. Horrocks, *Investigation of Cavitation in a Vertical Multi-Hole Diesel Injector.* 1999.

14. Roth, H., M. Gavaises, C. Arcoumanis, Cavitation *Initiation, its Development and Link with Flow Turbulence in Diesel Injector Nozzles*. SAE paper, 2002 (2002-01-0214).

15. Roth, H., *Experimental and Computational Investigation of Cavitation in Diesel Injector Nozzles*. Imperial College PhD Thesis., 2004.

16. Mitroglou, N., *Multi-hole Injectors for Direct-Injection Gasoline Engines PhD Thesis*, City University London, 2005.

17. Gavaises, M. and A. Andriotis, Cavitation *Inside Multi-hole Injectors for Large Diesel Engines and its Effects on the Near-nozzle Spray Structure*. SAE paper, 2006 (2006-01-1114).

18. Nouri, J.M., N. Mitroglou, N. Yan, C. Arcoumanis, *Internal flow and cavitation in a multi-hole injector for gasoline direct injection engines*. SAE paper, 2007.

19. Andriotis, A., M. Spathopoulou, M. Gavaises, *Effect of Nozzle Flow and Cavitation Structures on Spray Development in Low-speed Two-Stroke Diesel Engines*. International Council on Combustion Engines, CIMAC Congress, Vienna, 2007 (Paper 262).

20. Badock, C. , R. Wirth, A. Fath, A. Leipertz, *Investigation of cavitation in real size diesel injection nozzles*. International Journal of Heat and Fluid Flow, 1999.

21. Arcoumanis, C., H. Flora, M. Gavaises, M. Badami, *Cavitation in Real-Size, Multi-Hole Diesel Injector Nozzles*. SAE paper, 2000 (2000-01-1249).

22. Arcoumanis, C., M. Gavaises, H. Flora, H. Roth, *Visualisation of cavitation in diesel engine injectors*. Mecanique & Industries, 2001(5).

23. Blessing, M., G. Konig, C. Kruger, U. Michels, and V. Schwarz, *Analysis of Flow and Cavitation Phenomena in Diesel Injection Nozzles and its Effects on Spray and Mixture Formation*. SAE paper, 2003 (2003-01-1358).

24. Miranda, R., H. Chaves, U. Martin, F. Obermeier, *Cavitation in Transparent Real Size VCO Injection Nozzle*. ICLASS, 2003.

25. Roth, H., E. Giannadakis, M. Gavaises, C. Arcoumanis, K. Omae, I. Sakata, M. Nakamura, and H. Yanagihara, *Effect of Multi-Injection Strategy on Cavitation Development in Diesel Injector Nozzle Holes*. SAE paper, 2005 (2005-01-1237).

26. Gilles-Birth, I., M. Rechs, U. Spicher, and S. Bernhardt, *Experimental Investigation of the In-Nozzle Flow of Valve Covered Orifice Nozzles for Gasoline Direct Injection*. 7th International Symposium on Internal Combustion Diagnostics, Kurhaus Baden-Baden, 2006.

27. Li, L., *Experimental Study of Biodiesel Spay and Combustion Characteristics*. SAE paper, 2006.

28. Postrioti, L., C.N. Grimaldi, M. Ceccobello, and R. DiGioia, *Diesel Common Rail Injection System Behaviour with Different Fuels*. SAE paper, 2004 (2004-01-0029).